ORIGINAL PAPER

Fabrication and characterization of hydroxyapatite-strontium/polylactic acid composite for potential applications in bone regeneration

Ayodeji Nathaniel Oyedeji[1,2] · David Olubiyi Obada[1,2,3] ⬤ ·
Muhammad Dauda[1,4] · Laminu Shettima Kuburi[1,2] · Stefan Csaki[5] ·
Jakub Veverka[6]

Abstract

In this study, polylactic acid (PLA) was reinforced with hydroxyapatite (HAp) microparticles and strontium (Sr) powder via the melt extrusion/hot pressing manufacturing process to produce scaffolding materials with bone regeneration potentials. After the fabrication of the materials, the physico-chemical and mechanical characteristics were investigated. The morphology of the precursors for scaffold fabrication and the resulting composites was investigated. The structural characterization showed the semicrystalline nature of the PLA polymer and the characteristic reflections of HAp loading in the polymer matrix. The functional groups of the PLA matrix and the loaded variants showed the characteristic bands of HAp and Sr for the PLA-HAp and PLA-HAp-Sr scaffolding materials, respectively. Moreover, the physical property evaluation showed that with the addition of HAp, the porosity of the PLA-HAp scaffolds was reduced. However, the addition of Sr increased the porosity of the scaffolds, and this can possibly be ascribed to the grain refinement ability of strontium. The mechanical measurement data showed that the inclusion of Sr produced the maximum average Vickers hardness value of 49.1 HV. The composite scaffolds showed bioactivity potentials, thus, they can serve as suitable bone regeneration materials.

Keywords Polylactic acid · Hydroxyapatite · Strontium · Bone regeneration · Biomaterials

---

✉ David Olubiyi Obada
doobada@abu.edu.ng

Extended author information available on the last page of the article

Introduction

The present therapeutic options for treating bone abnormalities such as those associated with bone tissue loss owing to degenerative, surgical, or traumatic processes are current challenges faced by the global population's increasing age and life expectancy [1]. Bone tissue engineering as an alternative to traditional bone grafts is seen to be a viable technology for bone regeneration. Auto-, allo-, and xenografts are examples of the traditional bone grafts strategy for bone healing, but their use is hampered by several drawbacks, such as donor-site morbidity and pain, difficult graft resorption, lack of osteoinductive properties, immune rejection, and the risk of pathogen transfer. By implanting porous scaffolds that replicate the natural bone extracellular matrix (ECM) and combining them with osteogenic cells and morphogenic signals to encourage cell growth, proliferation, and differentiation, bone tissue engineering could alleviate the aforementioned challenges [2]. Out of the many synthetic materials used in bone substitute grafts, calcium phosphate (CaP) materials have gained widespread recognition. Hydroxyapatite (HAp), a member of the calcium phosphate group has chemical similarities with the inorganic component of the bone matrix. With about 60% of HAp being calcium phosphate, this has trigged intensive work to apply HAp as a bone substitution therapy for biomedical applications which includes suitable matrices to control drug release, in addition to its biocompatibility and remarkable osteoconduction. In addition, HAp is commonly used as coating implants and bone fillers. By reason of these and their relationship to bone cell biology, opportunities have opened for the use of HAp crystals to supplement application in bone regeneration. In fabricating hydrogels for biomedical applications, polylactic acid (PLA), a biodegradable thermoplastic aliphatic polyester has been widely used as a basic material for scaffolds in bone, cartilage, tendon, neural, and vascular regeneration for tissue engineering applications. As a biomaterial, it has been approved by the Food and Drug Administration (FDA) for direct contact with biological fluids and can be produced at a cheap cost using renewable resources such as corn and sugar beets [3]. Direct polycondensation of lactic acid and ring-opening polymerization of lactide, which is a cyclic dimer of lactic acid, are the two most common ways of producing PLA [4]. The properties of the polymer can be modified to the individual application by changing the starting composition [3]. PLA's properties are also influenced by the temperature at which it is processed in addition to its molecular weight [2].

PLA has been widely employed in the biomedical industry including suture, bone fixation material, drug delivery systems, and tissue engineering due to its biocompatibility, biodegradability, and acceptable mechanical properties [5]. PLA is also easily processed using a variety of methods allowing its degradation rate, physical qualities, and mechanical capabilities to be varied over a wide range by changing the molecular weight or copolymer ratio. The use of poly(d-lactic acid) (PDLA) in drug delivery systems due to its faster degradation rate, and the usage of poly(l-lactic acid) (PLLA) for load-bearing applications due to its superior mechanical qualities are only a few of the applications of PLA

and its various stereochemical variants [6]. PLA is also employed as a scaffold foundation material since it can be entirely degraded by random hydrolytic chain scission, resulting in lactic acid monomers that are excreted from the patient via the tricarboxylic acid cycle. Surface erosion where the breakdown occurs at the polymer–water interface, and bulk erosion, where degradation occurs uniformly throughout the polymer's surface are the ways in which PLA degradation occurs [7].

One of the key disadvantages of PLA is its low hydrophilicity with a water contact angle of roughly 80 degrees. This results in a lack of cell attachment and interaction between the polymer and the surrounding tissues as well as poor wetting qualities [12]. PLA bioactivity must be improved for it to be used in bone regeneration applications taking into account all of these features. The final degradation products of PLA are water and carbon dioxide which are not harmful to the human body. Hydroxyapatite (HAp) and other CaP compounds, as well as ceramic bioglasses are the biomaterials that have shown the most promising results in improving the bioactivity of PLA [13]. Ceramic additives added to the PLA matrix have been reported to improve the 3D structures' hydrophilicity, osteoconductivity, mineralization after implantation, and mechanical characteristics [2]. Furthermore, because of the basic character of bio-ceramic compounds, they act as buffers during the degradation process, preventing the formation of localized areas with an acidic environment that could trigger an inflammatory response [13]. HAp as a mineral component inside the bones and teeth of humans enable the incorporation of various ionic substitutions. In recent times, doping on CaPs to increase the material performance has gained a lot of interest especially in bone diseases. The calcium ion is substituted by divalent ions such as Strontium ion (Sr^{2+}) which has been reported to increase the bioactivity in bone regeneration in vivo and in vitro [14].

To date, a good number of Sr-doped HAp biomaterials have been produced with different formulations. In these studies, the Sr^{2+} ions were introduced into the final HAp product using different techniques [14, 34–40]. The Sr ion has the potential of increasing bone formation but decreases bone resorption. Sr could be substituted through ion exchange in the HAp structure and these substitutions can be made to simulate the chemical composition of the human bone and improve the mechanical, antibacterial, and biological properties [41]. In addition, the presence of Sr creates larger distance of Sr-OH due to the superior ionic diameter in the bone mineral when compared with Ca-OH resulting in a decline in the crystallinity and the lattice energy. The alteration of the lattice parameter and the crystallinity might change the apatite structure [42] and it might as well improve the biological properties in vitro and in vivo [43]. In the same vein, some studies have considered the development of Sr-doped HAp/PLA biomaterial; however, these studies considered synthetic HAp [44, 45] with limited studies on naturally derived HAp.

The targeted design of scaffolds should mimic the extracellular matrix (ECM), hence, many facile methods have been employed to fabricate 3D fibrous structures which possess a high surface-area-to-volume ratio that is close in structure to the ECM with interconnected pore architectures [23–30]. The melt extrusion/hot pressing manufacturing method is a method of turning raw materials, usually containing a polymer substrate and plasticizer, into a product of uniform shape and density by

pushing them through a heated barrel at an enhanced controlled temperature and pressure [8, 9]. More conceptually and methodically, this process can be divided into four steps: (1) Extruder feeding through a feeder, (2) Mixing, grinding, particle size reduction, venting, and kneading, (3) Flow through the die, and (4) Extrusion from the die and downstream processing [10, 11]. To the best of our knowledge, the possibility of fabricating strontium-doped HAp loaded in a polymer matrix using the facile melt mixing/hot pressing method assisted with the solution gelation method for the fabrication of polymeric 3D scaffolds has not been investigated in detail.

Hence, the composite presented in this study is one example of adopting the two-step processing method (solution gelation and melt extrusion/hot press technique) for the fabrication of Sr-HAp/PLA composites. The novelty of this study is the synergy of naturally sourced HAp doped with Sr and loaded in a PLA matrix to produce cheap and clinically viable scaffolds. We hypothesize that combining naturally sourced HAp and doping same with Sr ions before eventually loading in the PLA matrix using the two-step processing technique will produce robust scaffolds that can mimic the ECM in vitro and in vivo. The materials characterization carried out to determine the influence of HAp and Sr ions on the properties of the PLA-reinforced scaffolds for possible biomedical applications are reported herein.

Materials and methods

Materials and development of samples

The materials used in this study consist of PLA purchased from Zhengzhou ORI Laboratory tools, China. Sr salt ($Sr(NO_3)_2$) was purchased from Sigma Aldrich, USA. The HAp powders were produced at the Multifunctional Materials Laboratory (MFML), Ahmadu Bello University, Zaria, Nigeria which has extensive experience in synthesizing biomaterials [15, 46–53]. The methodology employed in the development of the PLA-HAp and PLA-HAp-Sr scaffolds is shown in Fig. 1.

In the production of the PLA-HAp, and PLA-HAp-Sr scaffolds, the as-synthesized HAp was mixed with $Sr(NO_3)_2$ using the solution gelation method. Water was used to mix both precursors. The solution was subjected to magnetic stirring for 2 h with a stepwise increase in heat. Once the mixing process was completed, the gel was placed in an oven for 24 h at 60 °C [14]. The PLA in its as-purchased form (strands), the HAp, and Sr salts were extruded through the use of a two-roll melt extrusion machine at a temperature of 165 °C. The PLA-HAp scaffold consisted of 80 wt% PLA and 20 wt% HAp, while the PLA-HAp-Sr scaffold consisted of 80 wt% PLA, 18 wt% HAp, and 2 wt% Sr. The designation and composition of the composites fabricated are given in Table 1.

At the end of the melt extrusion process, the samples were further pressed to improve the solidification of the mix through the use of the electric hydraulic press with a pressure of 0.4 MN/m^2. The produced scaffolds are shown in Fig. 2.
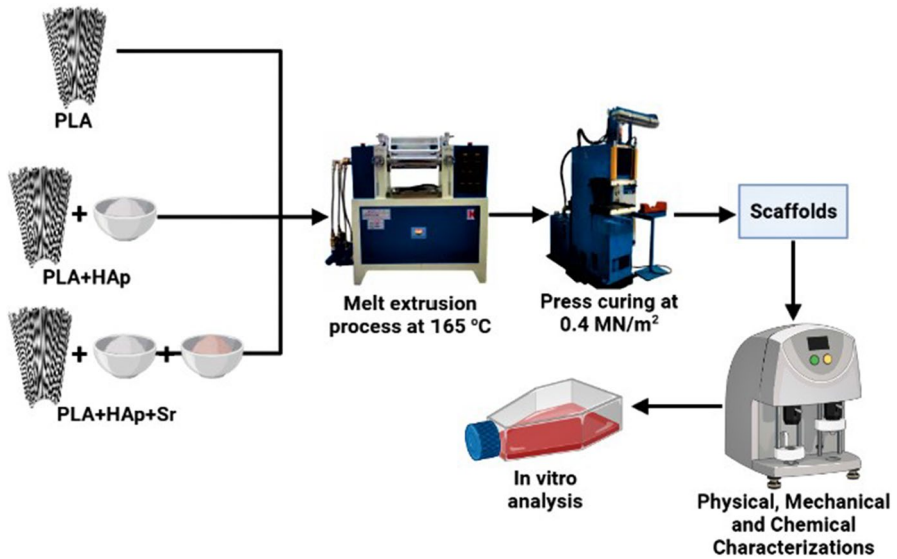
Fig. 1 Schematic showing the methodology for producing and testing the PLA-HAp-Sr scaffolds

Table 1 Designation and composition of composites fabricated

Sample	PLA (wt%)	HAp (wt%)	Sr (wt%)
PLA	100	–	–
PLA + HAp	80	20	–
PLA + HAp + Sr	80	18	2

Scanning electron microscopy (SEM)

SEM imaging was conducted to reveal the morphology of the polymer composite precursors and the fabricated composites. For HAp (raw and sintered variants), the microstructure of the samples was studied on an ultra-high vacuum and high-resolution FEI Xl-30 SEM operated at 5 kV. The samples were gold-sputtered and viewed at low magnification (2000 X) and high magnification (15,000 X) to reveal intrinsic features not shown during the imaging at low magnification. For the polymer precursors and composites, a high-resolution SEM machine was used. The SEM machine was operated at an accelerating voltage of 20 kV and the

Fig. 2 Developed polymeric scaffolds
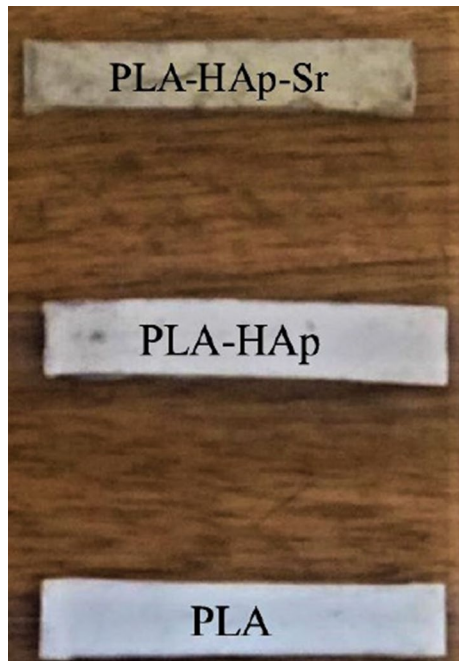
imaging was done at a low magnification (1000 X) and relatively higher magnification (3000 X) to reveal the intrinsic features not shown at lower magnifications.

XRD analysis

To investigate the structure and phases present in the developed polymeric scaffolds, X-ray powder diffraction (XRD) patterns were collected using a Rigaku Miniflex Diffractometer operating on a copper tube ($\lambda = 1.5418A$) generated at a voltage of 40 kV and a current of 30 mA. The goniometer was set at a scan rate of 0.033°/s over a 2θ range of 5–80°. This was followed by matching the obtained XRD data with standard PDF cards.

FTIR analysis

ATR- Fourier Transform-Infrared analysis was used to evaluate the functional groups of the developed PLA, PLA-HAp, and PLA-HAp-Sr scaffolds. For each scaffold, about 2 g was inserted in the PerkinElmer Frontier FTIR machine (1

wt.% particulate specimen and 99 wt.% KBr). The outputs were the scaffolds' FTIR spectra from 400 to 4000 cm^{-1}.

Hardness

The mechanical property of the developed polymeric scaffolds was evaluated in terms of their hardness. The hardness of the scaffolds was obtained using Vickers's micro-hardness tester. The tester consists of an indenter with an indenting load of 300 g and an indenting time of 10 s.

Volumetric porosity

The volumetric porosity of the developed polymeric scaffolds was determined using the Archimedes principle as stated by Bose and Daz [16]. In this methodology, the weights of the developed scaffolds were measured as dry weight (W_1), thereafter, the scaffolds were soaked in water for 24 h, after which the samples were wiped clean of excess water and weighed as wet weight (W_2). The volumetric porosity was obtained using the expression in Eq. (1).

$$\text{Porosity} = \frac{W_2 - W_1}{\rho * V} \tag{1}$$

where V is the volume of the developed scaffolds (as a function of the diameter and height), and ρ is the density of water.

In vitro analysis and post-in vitro hardness measurements

To study the physiological stability of the developed scaffolds, the scaffolds were soaked in Dulbecco's phosphate-buffered saline (PBS) solution covered in plastic containers containing 50 ml of the solution and conditioned at body temperature (37 °C) for up to 21 days. The scaffolds immersed were assessed post-immersion in the PBS using hardness measurements. Furthermore, the weight of the scaffolds and the pH were obtained for each day of the experimentation using the weighing scale and pH meter, respectively.

Statistical analysis of the mechanical property

The one-way analysis of variance (ANOVA) statistical test was carried out using the IBM SPSS 26 software. This analysis was carried out to determine the effect of HAp and Sr doping on the hardness of the developed scaffolds in terms of the comparison of the mean of the hardness values obtained for the scaffolds at a significant level of 0.05.
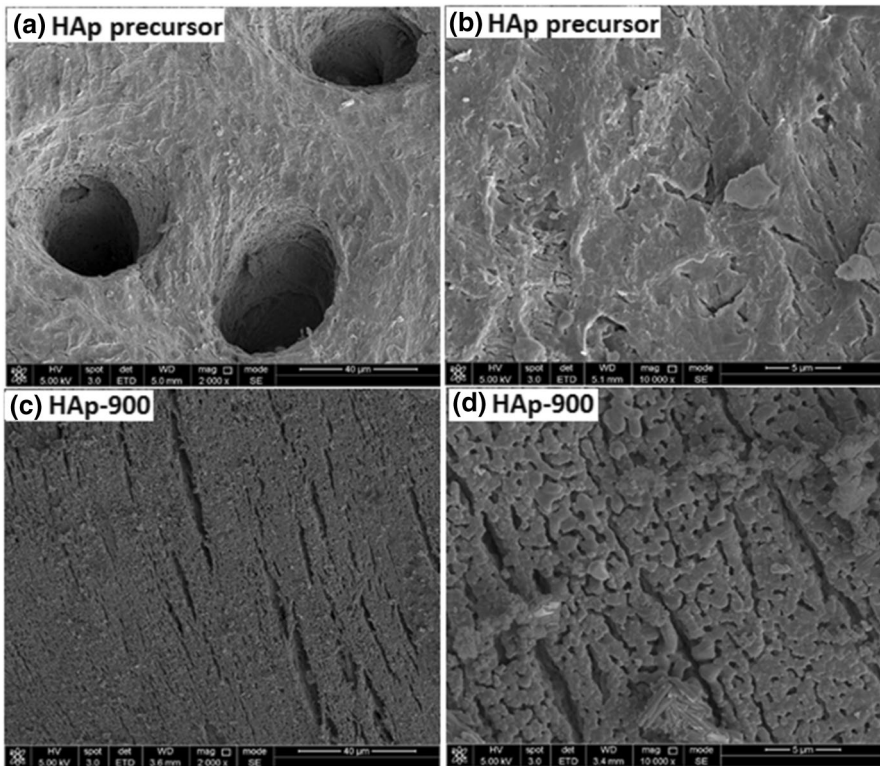
Fig. 3 SEM micrographs of HAp precursor **a** 2000×; **b** 15000×, and HAp-900 **c** 2000×; **d** 15000×

Results and discussion

SEM analysis

The SEM images of the HAp precursors and sintered samples are presented in Fig. 3. The gradients in the morphological features before and after heat treatment such as the formation of hollow surfaces was noticeable on the microstructure of the HAp at low magnification. For the sintered HAp variant, particles that are discrete in nature and the densely packed surface can be related to the removal of organic residues from the HAp precursors during sintering which was also described in a study carried out elsewhere [31]. The sintered HAp sample showed grain structures with clear grain boundaries. In addition, the interconnectivity between the grain structure becomes closer to each other at both low and higher magnifications and this defines the initiation of a crystalline grain structure of HAp [32].

Figure 4 shows the neat PLA which exhibits uniform and slightly rough (at higher magnification) and smooth (lower magnification) fracture surfaces [33]. For the SEM images at both magnifications of PLA-HAp, it is observed that the
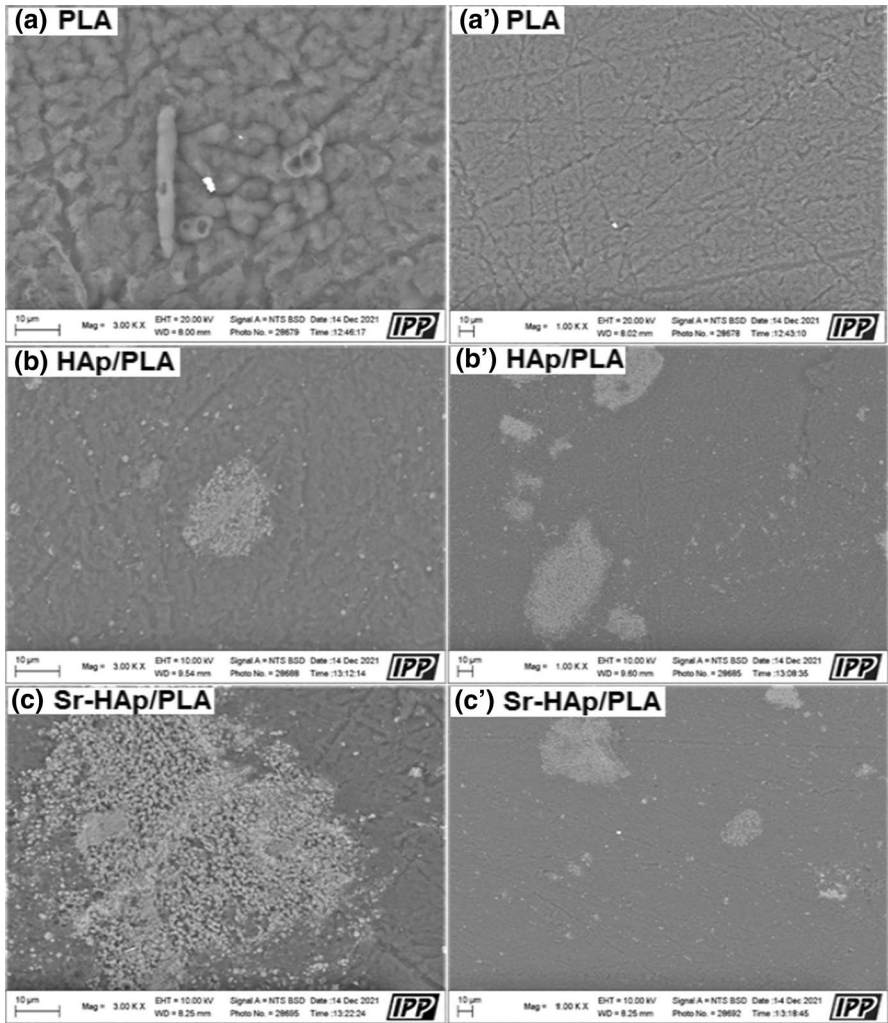
Fig. 4 SEM images of PLA, PLA-HAp, and PLA-HAp-Sr composite **a** PLA; **b** PLA-HAp **c** PLA-HAp-Sr at higher magnification (3000×) and **a′** PLA; **b′** PLA-HAp **c′** PLA-HAp-Sr at lower magnification (1000×)

HAp crystals are embedded in the matrix. This is more obvious in the imaging taken at higher magnification. For the PLA-HAp-Sr images (especially for the image at higher magnification), the quantity of crystals embedded in the PLA matrix is increased and this suggests the inclusion of both Sr ions and HAp in the PLA matrix. The inclusion of HAp and Sr played a role in controlling the morphology of the composites and it has been reported that the presence of these powders in the PLA matrix can improve the biocompatibility of polymeric scaffolds [14, 49].
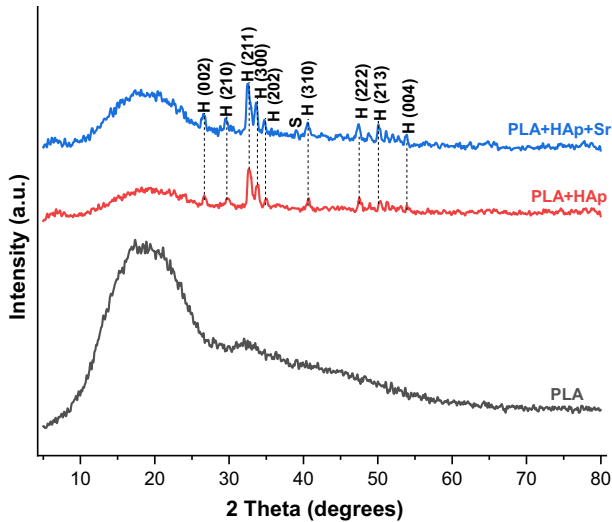
Fig. 5 XRD of PLA, PLA-HAp, and PLA-HAp-Sr scaffolds

XRD analysis

The XRD analysis of the PLA scaffolds (Fig. 5) within the 2-theta range of 5 and 80° showed a semicrystalline structure with noticeable reflection at the Bragg angle of 19.01° [17]. Furthermore, the XRD analysis of PLA-HAp and PLA-HAp-Sr scaffolds was matched with ICCD PDF card no 96-900-1234. The results showed that the PLA-HAp and PLA-HAp-Sr scaffolds had reflections
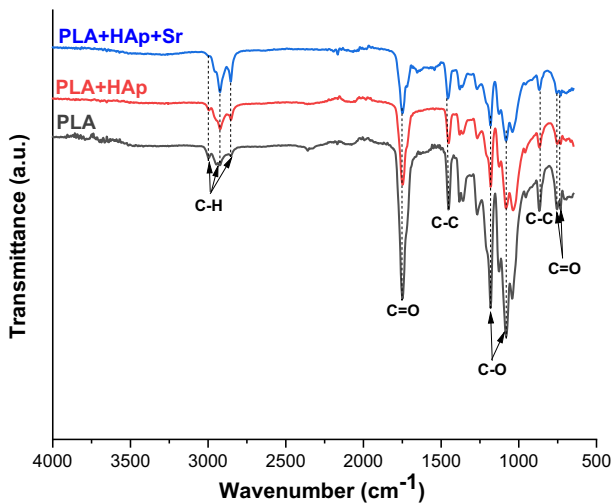

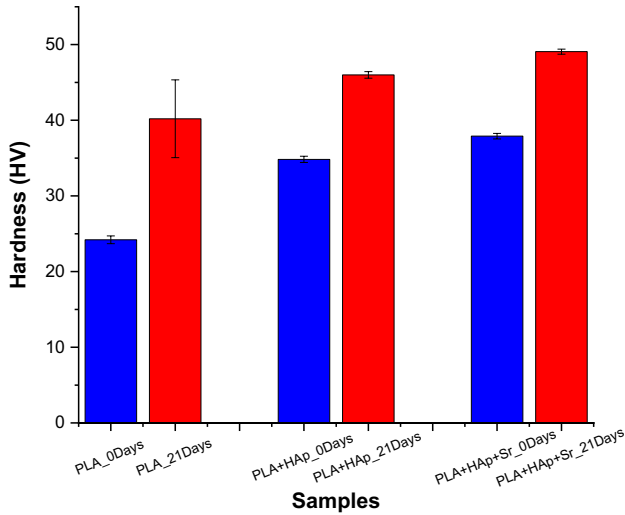**Fig. 6** FTIR of PLA, PLA-HAp, and PLA-HAp-Sr samples

Fig. 7 Hardness of PLA, PLA-HAp, and PLA-HAp-Sr Samples pre and post-in vitro

Table 2 One-Way ANOVA on the effect of HAp and Sr on the hardness of the developed scaffolds based on the variance, mean square, F-value, and p-value

	Sum of squares	df	Mean Square	F	Sig
Between groups	310.162	2	155.081	276.382	.000
Within groups	3.367	6	.561		
Total	313.529	8			

corresponding to HAp (indicated as H in Fig. 5) with miller planes of (002), (210), (211), (300), (202), (310), (222), (213), and (004) at the 2-theta angle of 26, 29, 32, 33, 34.26, 40.14, 47, 49, and 53°, respectively. A reflection corresponding to $SrCO_3$ (indicated as S in Fig. 5) was observed on the PLA-HAp-Sr at about 2-theta angle of 40°. The reflections in the PLA-HAp-Sr seems to show higher intensity which can be attributed to the effect of doping with Sr [14].

FTIR analysis

The FTIR spectra of the developed PLA, PLA-HAp, and PLA-HAp-Sr scaffolds are given in Fig. 6. The characteristic stretch vibrations of the carbonyl group band (C=O) and (C–O) bond of the ester structure in PLA appear at 1755 cm^{-1} and in the range of 1613 and 1183 cm^{-1} [17]. Also, the FTIR spectrum shows

that the carbonyl group band reduces in the case of PLA-HAp and PLA-HAp-Sr. This can be attributed to the inclusion of HAp and Sr in the composite mix.

Hardness

The mechanical property of the developed scaffolds in terms of their Vickers hardness is shown in Fig. 7. It was observed that before in vitro analysis, the Vickers hardness of the scaffolds increased based on the doping with HAp and Sr. This can be attributed to the reinforcing properties of these dopants as the inclusion of Sr gave the maximum average hardness value of 49.1 HV, which is higher than the hardness value required for cortical and cancellous bones of 26.04 HV and 22.92 HV, respectively [18].

The analysis of variance (ANOVA) corresponding to the three groups of the developed scaffolds before in vitro analysis is depicted in Table 2. From the result obtained, it was observed that the obtained Fo value of 276.382 is greater than the cut-off value of 5.143 which is from the F distribution with 2 and 6 degrees of freedom, and a significance level of 0.05. Therefore, the null hypothesis that states that the mean levels, as obtained from the hardness test experiments conducted before in vitro analysis are the same is rejected. From this analysis, it can be stated that the addition of HAp and Sr has significant effects on the hardness value of the developed scaffolds.
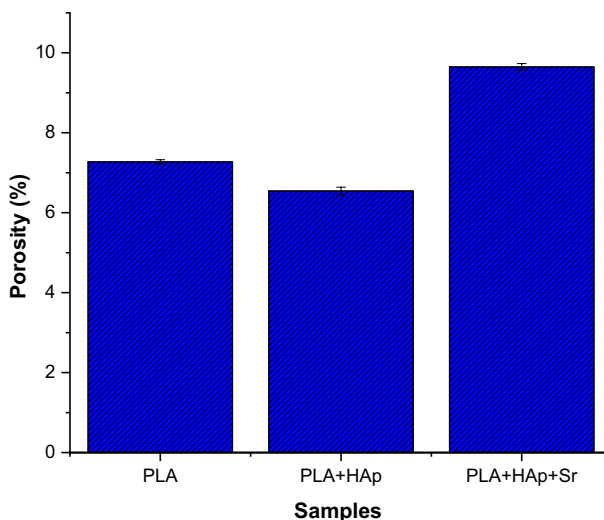
Fig. 8 Volumetric porosity of the PLA, PLA-HAp, and PLA-HAp-Sr scaffolds
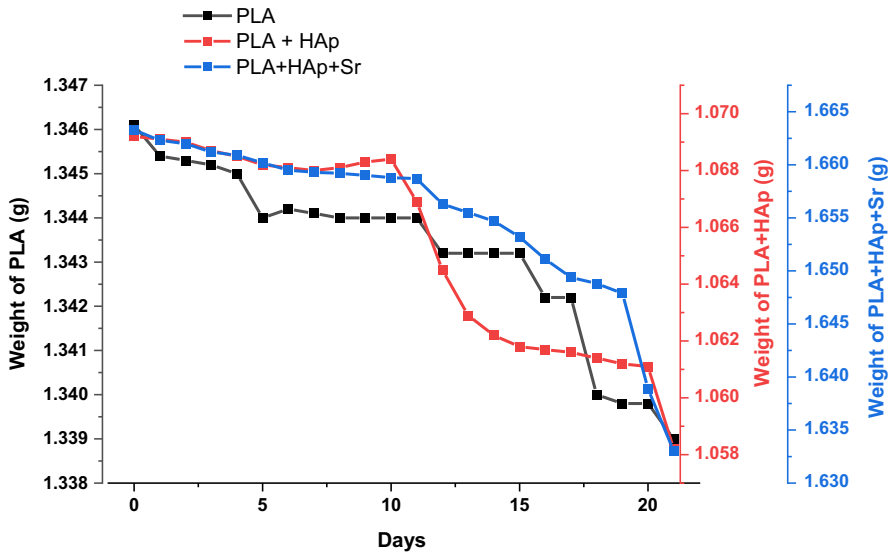
**Fig. 9** Weight reduction in PLA, PLA-HAp, and PLA-HAp-Sr samples in vitro

Furthermore, post-in vitro hardness results showed that for the developed scaffolds, the hardness increases. This can be ascribed to the continuity of the setting response of the developed scaffolds [19]. Additional clinical studies are required to analyze the adaptation of the scaffolds to confirm the long-term adaptability per the regeneration of critical-sized defects.

Volumetric porosity

Figure 8 shows the volumetric porosity of the developed scaffolds. The result showed that the PLA-HAp-Sr scaffold had the highest porosity of 9.65%, while the PLA-HAp scaffold manifested the lowest porosity which is almost the same value as the neat PLA scaffold. It is safe to say that the inclusion of HAp and Sr will serve as fillers in the PLA matrix, however, studies have proven that Sr tends to improve the porosity of materials due to its grain refinement ability [20]. Due to the relatively low porosity of the scaffolds obtained from this production method, its area of usage should be advised as stipulated for acceptable porosity levels for cortical bones [21].

In vitro analysis

Figure 9 shows the weight reduction in the developed scaffolds as a result of degradation when immersed in phosphate buffer saline (PBS) for 21 days. The result shows a similar degradation trend of the developed scaffolds for the study period.
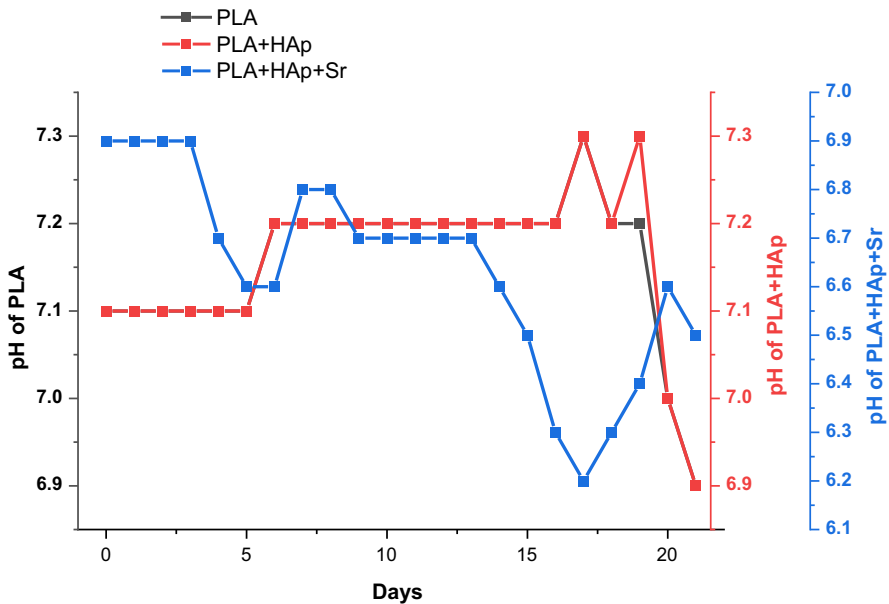
Fig. 10 pH profiles of PLA, PLA-HAp, and PLA-HAp-Sr samples in vitro

The degradation process is initially caused by the diffusion of the PBS solution into the amorphous regions of the PLA matrix, thereby resulting in degradation in these regions. This result shows the suitability of the developed scaffolds for bone regeneration since the scaffolds are biodegradable with the PLA-HAp-Sr scaffold showing more stability in terms of the degradation rate.

Figure 10 shows the pH profiles of the developed scaffolds during the degradation process in PBS solution (pH = 7.1). Noticeable pH changes were not observed till after day 3 of the experimental study, and afterwards, changes were noticed in the pH of PLA and PLA-HAp until it reduced to its lowest pH value of 6.9 after 21 days. However, the pH of PLA-HAp-Sr had its lowest value on day 17 and increased to a range of 6.5–6.6. According to the findings of Chu et al. [22], it was reported that a pH value of about 6.5 exhibits a more drug release ability of scaffolds. Hence, since the pH value of the developed PLA-HAp-Sr is close to 6.5, it can be hypothesized that the scaffold can be useful for drug delivery applications.

Conclusion

With the application of the melt extrusion/hot pressing method for the development and characterization of the PLA, PLA-HAp, and PLA-HAp-Sr scaffolds, the suitability of the scaffolds as bone regenerative materials was investigated. The results of the morphological and structural characterization showed variations in morphology as crystals were embedded in the PLA matrix of the composite scaffolds. In

addition, structurally, the semicrystalline nature of the PLA polymer and the characteristic reflections of HAp loading in the polymer matrix was noticed. The physical property evaluation showed that with the addition of HAp, the porosity of the PLA-HAp scaffolds was reduced. However, the addition of Sr increased the porosity of the scaffolds. The mechanical property showed that the inclusion of Sr gave the maximum average Vickers hardness value of 49.1 HV, which is higher than the Vickers hardness value for implantable materials in the cortical and cancellous bone regions. In vitro experiments showed the degradability of the scaffolds, with the pH of PLA-HAp-Sr within a range of 6.5 – 6.6 after 17 days, though further analysis can be conducted using cell culture assays. These results indicate that the scaffolds are promising as bone regeneration materials.

References

1. Improta G, Balato G, Romano M, Ponsiglione AM, Raiola E, Russo MA, Cesarelli M (2017) Improving performances of the knee replacement surgery process by applying DMAIC principles. J Eval Clin Pract 23(6):1401–1407
2. Donate R, Monzón M, Alemán-Domínguez ME (2020) Additive manufacturing of PLA-based scaffolds intended for bone regeneration and strategies to improve their biological properties. E-Polymers 20(1):571–599
3. Gritsch L, Conoscenti G, La Carrubba V, Nooeaid P, Boccaccini AR (2019) Polylactide-based materials science strategies to improve tissue-material interface without the use of growth factors or other biological molecules. Mater Sci Eng, C 94:1083–1101
4. Akindoyo JO, Beg MD, Ghazali S, Heim HP, Feldmann M (2017) Effects of surface modification on dispersion, mechanical, thermal, and dynamic mechanical properties of injection-moulded PLA-hydroxyapatite composites. Compos A Appl Sci Manuf 103:96–105
5. Singhvi MS, Zinjarde SS, Gokhale DV (2019) Polylactic acid: synthesis and biomedical applications. J Appl Microbiol 127(6):1612–1626
6. Farah S, Anderson DG, Langer R (2016) Physical and mechanical properties of PLA, and their functions in widespread applications—A comprehensive review. Adv Drug Deliv Rev 107:367–392
7. Reddy M, Ponnamma D, Choudhary R, Sadasivuni KK (2021) A comparative review of natural and synthetic biopolymer composite scaffolds. Polymers 13(7):1105
8. Maniruzzaman M, Douroumis D, Joshua S, Martin J (2012) Hot-melt extrusion (HME): from process to pharmaceutical applications. In: Sezer A D (ed) Recent Advances in Novel Drug Carrier Systems. InTech. https://doi.org/10.5772/51582
9. Manavitehrani I, Fathi A, Badr H, Daly S, Negahi Shirazi A, Dehghani F (2016) Biomedical applications of biodegradable polyesters. Polymers 8(1):20
10. Zheng Y, Pokorski JK (2021) Hot-melt extrusion: an emerging manufacturing method for slow and sustained protein delivery. Wiley Interdiscip Rev: Nanomed Nanobiotechnol 13(5):e1712
11. Ouyang Q, Feng X, Kuang S, Panwar N, Song P, Yang C, Wang ZL (2019) Self-powered, on-demand transdermal drug delivery system driven by triboelectric nanogenerator. Nano Energy 62:610–619
12. Shen P, Moriya A, Rajabzadeh S, Maruyama T, Matsuyama H (2013) Improvement of the antifouling properties of poly (lactic acid) hollow fibre membranes with poly (lactic acid)–polyethylene glycol–poly (lactic acid) copolymers. Desalination 325:37–39
13. Guvendiren M, Molde J, Soares RM, Kohn J (2016) Designing biomaterials for 3D printing. ACS Biomater Sci Eng 2(10):1679–1693

14. Obada DO, Salami KA, Oyedeji AN, Fasanya OO, Suleiman MU, Ibisola BA, Dauda ET (2021) Solution combustion synthesis of strontium-doped hydroxyapatite: effect of sintering and low compaction pressure on the mechanical properties and physiological stability. Mater Lett 304:130613

15. Obada DO, Dauda ET, Abifarin JK, Dodoo-Arhin D, Bansod ND (2020) Mechanical properties of natural hydroxyapatite using low cold compaction pressure: effect of sintering temperature. Mater Chem Phys 239:122099

16. Bose S, Das C (2013) Preparation and characterization of low-cost tubular ceramic support membranes using sawdust as a pore-former. Mater Lett 110:152–155

17. Leyva-Verduzco AA, Castillo-Ortega MM, Chan-Chan LH, Silva-Campa E, Galaz-Méndez R, Vera-Graziano R, Santos-Sauceda I (2020) Electrospun tubes based on PLA, gelatin, and genipin in different arrangements for blood vessel tissue engineering. Polym Bull 77(11):5985–6003

18. Zhang Z, Li S, Wang J (2019) Measurement of micro-hardness of the human lower cervical vertebrae in vitro. Chin J Anat Clin 24(5):425–429

19. Poskus LT, Latempa AMA, Chagas MA, Silva EMD, Leal MPDS, Guimarães JGA (2009) Influence of post-cure treatments on hardness and marginal adaptation of composite resin inlay restorations: an in vitro study. J Appl Oral Sci 17:617–622

20. Şevik H, Kurnaz SC (2014) The effect of strontium on the microstructure and mechanical properties of Mg–6Al–0.3 Mn–03 Ti–1Sn. J Magnes Alloys 2(3):214–219

21. Pandithevan P, Saravana Kumar G (2009) Personalized bone tissue engineering scaffold with controlled architecture using fractal tool paths in layered manufacturing. Virtual Phys Prototyp 4(3):165–180

22. Chu L, Gao H, Cheng T, Zhang Y, Liu J, Huang F, Liu J (2016) A charge-adaptive nanosystem for prolonged and enhanced in vivo antibiotic delivery. Chem Commun 52(37):6265–6268

23. Chang C, Peng N, He M, Teramoto Y, Nishio Y, Zhang L (2013) Fabrication and properties of chitin/hydroxyapatite hybrid hydrogels as scaffold nano-materials. Carbohyd Polym 91(1):7–13

24. Maji S, Agarwal T, Das J, Maiti TK (2018) Development of gelatin/carboxymethyl chitosan/nano-hydroxyapatite composite 3D macroporous scaffold for bone tissue engineering applications. Carbohyd Polym 189:115–125

25. Wüst S, Godla ME, Müller R, Hofmann S (2014) Tunable hydrogel composite with two-step processing in combination with innovative hardware upgrade for cell-based three-dimensional bioprinting. Acta Biomater 10(2):630–640

26. Huang Y, Zhang X, Wu A, Xu H (2016) An injectable nano-hydroxyapatite (n-HA)/glycol chitosan (G-CS)/hyaluronic acid (HyA) composite hydrogel for bone tissue engineering. RSC Adv 6(40):33529–33536

27. Saravanan S, Chawla A, Vairamani M, Sastry TP, Subramanian KS, Selvamurugan N (2017) Scaffolds containing chitosan, gelatin and graphene oxide for bone tissue regeneration in vitro and in vivo. Int J Biol Macromol 104:1975–1985

28. Tripathi A, Saravanan S, Pattnaik S, Moorthi A, Partridge NC, Selvamurugan N (2012) Bio-composite scaffolds containing chitosan/nano-hydroxyapatite/nano-copper–zinc for bone tissue engineering. Int J Biol Macromol 50(1):294–299

29. Nam J, Huang Y, Agarwal S, Lannutti J (2007) Improved cellular infiltration in electrospun fiber via engineered porosity. Tissue Eng 13(9):2249–2257

30. Dhand C, Ong ST, Dwivedi N, Diaz SM, Venugopal JR, Navaneethan B, Lakshminarayanan R (2016) Bio-inspired in situ crosslinking and mineralization of electrospun collagen scaffolds for bone tissue engineering. Biomaterials 104:323–338

31. Ooi CY, Hamdi M, Ramesh S (2007) Properties of hydroxyapatite produced by annealing of bovine bone. Ceram Int 33(7):1171–1177

32. Lowe B, Venkatesan J, Anil S, Shim MS, Kim SK (2016) Preparation and characterization of chitosan-natural nano hydroxyapatite-fucoidan nanocomposites for bone tissue engineering. Int J Biol Macromol 93:1479–1487

33. Zhang X, Chen L, Mulholland T, Osswald TA (2019) Characterization of mechanical properties and fracture mode of PLA and copper/PLA composite part manufactured by fused deposition modeling. SN Appl Sci 1(6):1–12

34. Leroux L, Lacout JL (2001) Preparation of calcium strontium hydroxyapatites by a new route involving calcium phosphate cements. J Mater Res 16(1):171–178

35. Tadier S, Bareille R, Siadous R, Marsan O, Charvillat C, Cazalbou S, Combes C (2012) Strontium-loaded mineral bone cements as sustained release systems: compositions, release properties, and effects on human osteoprogenitor cells. J Biomed Mater Res B Appl Biomater 100(2):378–390

36. Wu T, Yang S, Lu T, He F, Zhang J, Shi H, Ye J (2019) Strontium ranelate simultaneously improves the radiopacity and osteogenesis of calcium phosphate cement. Biomed Mater 14(3):035005

37. No YJ, Xin X, Ramaswamy Y, Li Y, Roohaniesfahani S, Mustaffa S, Zreiqat H (2019) Novel injectable strontium-hardystonite phosphate cement for cancellous bone filling applications. Mater Sci Eng C 97:103–115

38. Lode A, Heiss C, Knapp G, Thomas J, Nies B, Gelinsky M, Schumacher M (2018) Strontium-modified premixed calcium phosphate cements for the therapy of osteoporotic bone defects. Acta Biomater 65:475–485

39. Kaygili O, Keser S, Kom M, Eroksuz Y, Dorozhkin SV, Ates T, Yakuphanoglu F (2015) Strontium substituted hydroxyapatites: synthesis and determination of their structural properties, in vitro and in vivo performance. Mater Sci Eng C 55:538–546

40. Sun L, Li T, Yu S, Mao M, Guo D (2021) A novel fast-setting strontium-containing hydroxyapatite bone cement with a simple binary powder system. Front Bioeng Biotechnol 9:168

41. Xue W, Hosick HL, Bandyopadhyay A, Bose S, Ding C, Luk KDK, Lu WW (2007) Preparation and cell–materials interactions of plasma sprayed strontium-containing hydroxyapatite coating. Surf Coat Technol 201(8):4685–4693

42. Li ZY, Lam WM, Yang C, Xu B, Ni GX, Abbah SA, Lu WW (2007) Chemical composition, crystal size and lattice structural changes after incorporation of strontium into biomimetic apatite. Biomaterials 28(7):1452–1460

43. Li Y, Li Q, Zhu S, Luo E, Li J, Feng G, Hu J (2010) The effect of strontium-substituted hydroxyapatite coating on implant fixation in ovariectomized rats. Biomaterials 31(34):9006–9014

44. Ge M, Ge K, Gao F, Yan W, Liu H, Xue L, Zhang J (2018) Biomimetic mineralized strontium-doped hydroxyapatite on porous poly (l-lactic acid) scaffolds for bone defect repair. Int J Nanomed 13:1707

45. Melo P, Naseem R, Corvaglia I, Montalbano G, Pontremoli C, Azevedo A, Fiorilli S (2020) Processing of Sr^{2+} containing Poly L-lactic acid-based hybrid composites for additive manufacturing of Bone Scaffolds. Front Mater 7:413

46. Akpan ES, Dauda M, Kuburi LS, Obada DO (2021) Box-Behnken experimental design for the process optimization of catfish bones derived hydroxyapatite: a pedagogical approach. Mater Chem Phys 272:124916

47. Osuchukwu OA, Salihi A, Abdullahi I, Obada DO (2022) Synthesis and characterization of sol–gel derived hydroxyapatite from a novel mix of two natural biowastes and their potentials for biomedical applications. Mater Today Proc. https://doi.org/10.1016/j.matpr.2022.04.696

48. Osuchukwu OA, Salihi A, Abdullahi I, Obada DO (2022) Experimental data on the characterization of hydroxyapatite produced from a novel mixture of biowastes. Data Brief 42:108305

49. Akpan ES, Dauda M, Kuburi LS, Obada DO, Dodoo-Arhin D (2020) A comparative study of the mechanical integrity of natural hydroxyapatite scaffolds prepared from two biogenic sources using a low compaction method. Res Phys 17:103051

50. Akpan ES, Dauda M, Kuburi LS, Obada DO (2020) A facile synthesis method and fracture toughness evaluation of catfish bones-derived hydroxyapatite. MRS Adv 5(26):1357–1366. https://doi.org/10.1557/adv.2020.172

51. Akpan ES, Dauda M, Kuburi LS, Obada DO, Bansod ND, Dodoo-Arhin D (2020) Hydroxyapatite ceramics prepared from two natural sources by direct thermal conversion: from material processing to mechanical measurements. Mater Today Proc 38:2291–4

52. Obada DO, Dauda ET, Abifarin JK, Bansod ND, Dodoo-Arhin D (2020) Mechanical measurements of pure and kaolin reinforced hydroxyapatite-derived scaffolds: a comparative study. Mater Today Proc. 38:2295–300

53. Obada DO, Osseni SA, Sina H, Salami KA, Oyedeji AN, Dodoo-Arhin D, Bansod ND et al (2021) Fabrication of novel kaolin-reinforced hydroxyapatite scaffolds with robust compressive strengths for bone regeneration. Appl Clay Sci 215:106298

Publisher's Note Springer Nature remains neutral with regard to jurisdictional claims in published maps and institutional affiliations.

Authors and Affiliations

Ayodeji Nathaniel Oyedeji[1,2] · **David Olubiyi Obada**[1,2,3] (iD) ·
Muhammad Dauda[1,4] · **Laminu Shettima Kuburi**[1,2] · **Stefan Csaki**[5] ·
Jakub Veverka[6]

1   Department of Mechanical Engineering, Ahmadu Bello University, Zaria, Nigeria

2   Multifunctional Materials Laboratory, Shell Office Complex, Department of Mechanical
      Engineering, Ahmadu Bello University, Zaria, Nigeria

3   Africa Centre of Excellence on New Pedagogies in Engineering Education, Ahmadu Bello
      University, Zaria, Nigeria

4   Air Force Institute of Technology, Nigerian Air Force Base, Kaduna, Nigeria

5   Department of Physics, Constantine the Philosopher University in Nitra, Nitra, Slovakia

6   Institute of Plasma Physics, The Czech Academy of Sciences, Prague, Czech Republic